Erschienen in: Seventeenth European Photovoltaic Solar Energy Conference : proceedings of the international conference held in Munich, Germany, 22 - 26, October 2001 ; Vol. 2 / McNelis, Bernard et al. (Hrsg.). - München [u.a.] : WIP-Renewable Energies [u.a.], 2001. - S. 1723-1726. - ISBN 3-936338-07-8

Preprint 17th European Photovoltaic Solar Energy Conference, Munich, Germany, 22-26 October 2001

INVESTIGATION OF THE LOCAL MINORITY CHARGE CARRIER DIFFUSION CONSTANTS OF DIFFERENT SILICON MATERIALS

D. Sontag, G. Hahn, P. Fath, E. Bucher
Universität Konstanz, Fachbereich Physik, Fach X916, 78457 Konstanz, Germany
Tel.: +49-7531-88-2132, Fax: +49-7531-88-3895
E-mail: detlef.sontag@uni-konstanz.de

ABSTRACT: The diffusion constant of the minority charge carriers D_n is an important parameter in photovoltaics. Nevertheless it is hard to detect. One method introduced by Stevens and Green delivers the integral value of D_n only for silicon materials with large diffusion lengths. In this paper a new method is introduced to determine D_n locally resolved and mapped in two dimensions. For that purpose the local bulk diffusion length L_{diff}, which can be calculated from LBIC (**L**aser **B**eam **I**nduced **C**urrent) measurements, has been combined with the local bulk lifetime τ_b received by µ-PCD (Microwave-detected **P**hoto **C**onductance **D**ecay) measurements. We evaluated the diffusion constants of the minority charge carriers for different multicrystalline p-type silicon materials with a resolution of 100 µm. As τ_b is mainly correlated to the amount of recombination centers while D_n is correlated to scattering centers, we were able to detect the position of both types of defects and also their correlation to each other. The measurements were carried out on solar cells before and after remote plasma hydrogen passivation in order to get an impression of the diffusion constant dependency on hydrogen incorporation.
Keywords: Minority Charge Carrier Diffusion Constant - 1: Diffusion Length - 2: Lifetime - 3

1. INTRODUCTION

The diffusion constants of crystalline silicon materials are generally considered to be constant over the whole volume of a solar cell. Common methods like Hall measurements deliver only the majority carrier diffusion constant integrated over the whole sample area. But the determination of the diffusion constant of minority charge carriers is rather difficult, although this parameter is actually more interesting in photovoltaics, as minority charge carriers are responsible for the current in a solar cell. There exists an integral method to determine D_n but only for materials with high lifetimes [1]. In this paper we introduce a method to overcome this problem and to determine D_n especially in different p-type materials with low diffusion lengths locally resolved and mapped in two dimensions.

2. EXPERIMANTAL APPROACH

The diffusion constant D_n is connected to the bulk diffusion length and the bulk lifetime by the equation

$$L_{diff} = \sqrt{D_n \cdot \tau_b}\ , \qquad (1)$$

i. e. we can derive D_n by performing an L_{diff} and a τ_b-measurement.

2.1 Measuring the Bulk Lifetime τ_b

An important parameter concerning the performance of solar cells are the bulk lifetimes τ_b of the minority charge carriers. Because of recombination at the surface of a wafer, always an effective lifetime τ_{eff} is measured, depending on the surface recombination velocity S, the diffusion constant D and the wafer thickness d.

$$\frac{1}{\tau_{eff}} = \frac{1}{\tau_b} + 2\frac{S}{d} \quad \text{for} \quad S << \frac{D}{d} \qquad (2)$$

The equation clarifies that by reducing S, τ_{eff} approaches τ_b. In our experiments the surfaces were passivated with Iodine-Ethanol. This kind of passivation reduces S to values of 150 cm/s [2], which is in our case sufficiently small for τ_{eff} to equal τ_b.

The lifetime has been measured using a µ-PCD, where a laser beam (λ = 905 nm, spotsize 800 µm) generates charge carriers. While these exess charge carriers recombinate, the conductivity changes exponentially with time. This can be measured by exposing the sample to microwaves and detecting the reflected signal as microwave reflection is a function of conductivity.

These measurements have been performed under low injection conditions[1]. The resulting lifetime map of an RGS (**R**ibbon **G**rowth on **S**ubstrate) [3] solar cell is shown in Fig. 1 (step size 100 µm). The front and backside contacts as well as the back surface field had to be removed, as they disturb the measurements and falsify the results. The emitter was also removed in order to perform the measurements with a well defined surface for passivation.

For EFG material with its huge variations in lifetime the mapping was more sophisticated. Several mappings with different time intervals had to be carried out. Afterwards these sets of data had to be combined in an appropriate way to receive a complete map [4].

[1] Low laser intensity

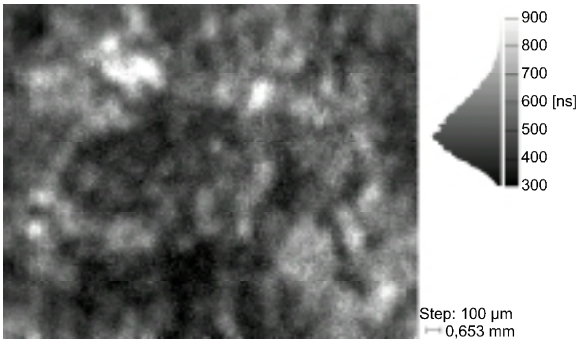

Figure 1: Lifetime measurement of a RGS solar cell. White regions correspond to high lifetimes.

2.2 Determination of L_{diff}

To derive an effective minority charge carrier diffusion length L_{eff} an LBIC measurement has been performed. Four laser beams with different wavelengths (635 nm, 835 nm, 910 nm and 980 nm) are generating charge carriers in the bulk of a solar cell. The resulting short circuit currents I_{SC} as well as the reflections are locally detected and mapped in two dimensions [5].

Once having measured the short circuit currents, the external quantum efficiency EQE(λ) can be calculated by the equation

$$EQE(\lambda) = SR_{ext}(\lambda)\frac{hc}{e\lambda} \tag{3}$$

with the external spectral response

$$SR_{ext} = \frac{I_{SC}(\lambda)}{F(\lambda)}, \tag{4}$$

the Planck constant h, the velocity of light c, the electron charge e, the wavelength λ and the illuminating light power $F(\lambda)$. As we are only interested in photons, which really enter the solar cell, we calculate the internal quantum efficiency $IQE(\lambda)$ according to

$$IQE(\lambda) = EQE(\lambda)\frac{1}{1-R(\lambda)} \tag{5}$$

with the reflectivity $R(\lambda)$. The absorption of light depends on the wavelength: the smaller the wavelength, the higher the absorption. Minority carriers generated deep in the bulk by long wavelength photons have to diffuse a longer distance to the collecting emitter than minority carriers generated by short wavelength photons. As a consequence the $IQE(\lambda)$ provides information about the diffusion length of the minority charge carriers. A high value of the $IQE(\lambda)$ for long wavelengths indicates large diffusion lengths. The corresponding equation proposed by Basore [6] for untextured solar cells in the range of wavelengths between 800 nm and 1000 nm is

$$\frac{1}{IQE(\lambda)} \approx 1 + \frac{1}{\alpha(\lambda)L_{eff}} \tag{6}$$

with the absorption coefficient $\alpha(\lambda)$. If the cell thickness d is larger than the bulk diffusion length L_{diff}, L_{eff} approximates L_{diff}.

The resulting L_{diff}-map for the RGS solar cell shown in Fig. 1 is presented in Fig. 2. The lateral resolution was adapted to the one of the µ-PCD.

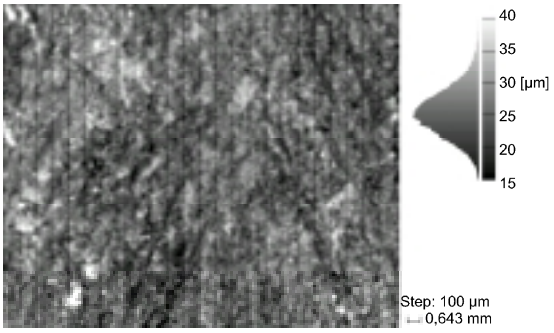

Figure 2: Map of the minority carrier diffusion lengths of the RGS solar cell shown in Fig. 1. A similar pattern can be observed.

The pattern looks quite the same like in the τ_b-map. Many regions with high L_{diff} correspond to regions with high lifetimes. The diffusion lengths for this material are typically in the range of 20 µm [7]. Comparing this value with the cell thickness of over 200 µm, the assumption $L_{diff} \approx L_{eff}$ is well satisfied.

2.3 Evaluating D_n

The diffusion constant was intended to be revealed before and after hydrogen passivation for the same solar cell. As a consequence the following process sequence had to be carried out:

1. LBIC measurement: ➜ L_{diff} without H-Passivation
2. Hydrogen passivation
3. LBIC measurement: ➜ L_{diff} with H-Passivation
4. Etching of the front and backside contacts, the backsurface field and the emitter
5. µ-PCD measurement: ➜ τ_b with H-Passivation
6. Hydrogen effusion
7. µ-PCD measurement: ➜ τ_b without H-Passivation

After these measurements all needed data is obtained to reveal D_n. The only thing left to do is to combine the corresponding sets of data from above. Basically all values of L_{diff} have to be squared and then divided by the correlated τ_b-values according to eq. (1). Up to now the allignment of the two maps is performed manually but we are working on an automisation for a more accurate calculation.

The resulting D_n-map is shown in Fig. 3. Some patterns from Fig. 1 and 2 are still visible in the D_n-map but others vanished. The values are more or less homogenous over the whole solar cell. Nevertheless there are a few regions with appearently high D_n.

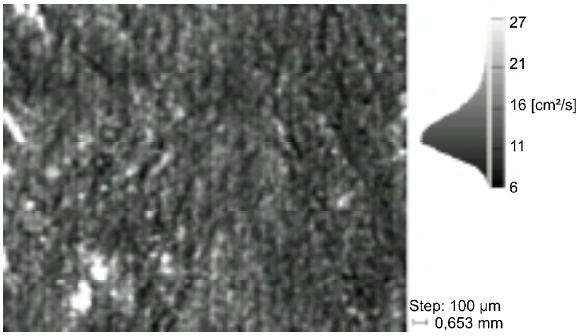

Figure 3: Map of the minority carrier diffusion constant of the RGS solar cell. In regions with values above 27 cm²/s current collecting inversion channels are present. Basore conditions (2D emitter) are not satisfied in these areas and the calculation of D_n delivers wrong values.

The maximum range is set to 27 cm²/s, which is the D_n value for monochrystalline silicon of the same resistivity [8], therefore all regions with higher diffusion constants (white areas) do not reveal the correct values. These regions indicate the presence of current collection channels as proposed by Häßler et al [9]. A schematic sketch is drawn in Figure 4.

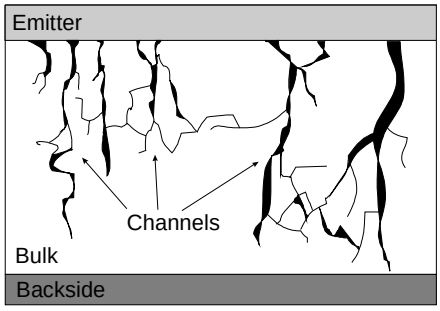

Figure 4: Sketch of the 3D emitter formed by a common 2D emitter and inversion channels (current collecting channels) as proposed by C. Häßler et al.

These current collecting channels, formed around dislocations [11], together with the diffused frontside emitter form a 3D emitter which does not satisfy Basore conditions. This results in an increase of the *IQE* in the long wavelength part of the spectrum corresponding to a high L_{eff} despite of an actually small L_{diff}. Therefore L_{eff} does not equal L_{diff} anymore and consequently the calculation results in too high values for D_n in these regions.

The determination of D_n has been carried out for different kinds of multicrystalline silicon materials before and after H-Passivation. The results are listed in Table I.

As mentioned before, our method of revealing D_n is only applicable for silicon materials with small diffusion lengths ($L_{diff} << d$). This prerequisition is not generally satisfied for all regions in EFG and Baysix material. As a consequence we had to exclude all good quality areas before deriving D_n. For Baysix material basically only areas around grain boundaries remained suitable. Concerning the H-Passivation a tendency to higher values is visible.

Table I: D_n peak values for different kinds of silicon materials. Difficulties appeared in evaluating D_n for EFG and Baysix.

	Before H-Passivation	After H-Passivation
RGS	9.7	11.3
EFG	9.2	11.1
BAYSIX	22	23

3. SCATTERING AND RECOMBINATION

Scattering and recombination both have a major influence on the performance of a solar cell. Scattering defects are slowing down electrons on their way to the pn-junction so they are a limiting factor for D_n. On the other hand recombination centers are reducing the lifetime of charge carriers.

We now focused on the question, if these mechanisms are somehow correlated or not. For easier examination of τ_b and D_n the difference to their mean values have been calculated and are displayed in Figure 5a and b respectively.

Dark regions in Figure 5a indicate reduced lifetimes corresponding to many recombination centers, while dark regions in Figure 5b are correlated with low diffusion constants or many scattering centers. In Figure 5c the difference of the IQE (Internal Quantum Efficiency) to ist mean value is displayed, so the defect density is comparable directly with the cell performance.

There are four regions marked on the maps in Figure 5. Region 1 indicates an area with high diffusion constants i.e. reduced scattering centers and increased lifetimes, correlated to a low recombination tendency. The IQE is also increased in this area, which corresponds to the assumption, that low defect densities lead to high cell performance.

Region 2 marks an area with high diffusion constants connected with low lifetimes. In this area recombination is increased while scattering is decreased. But regarding the IQE there is no significant dependency of recombination centers.

In region 3 we can see low D_n correlated with high lifetimes. This area has an increased scattering density while recombination is reduced. The IQE is also high regardless of the increased scattering.

In region 4 finally we find low diffusion constants, low lifetimes and a low IQE. In this area scattering as well as recombination densities are increased.

Other noticeable regions like the one to the left of region 4 were neglected because these regions include inversion channels and are not suitable for our investigation.

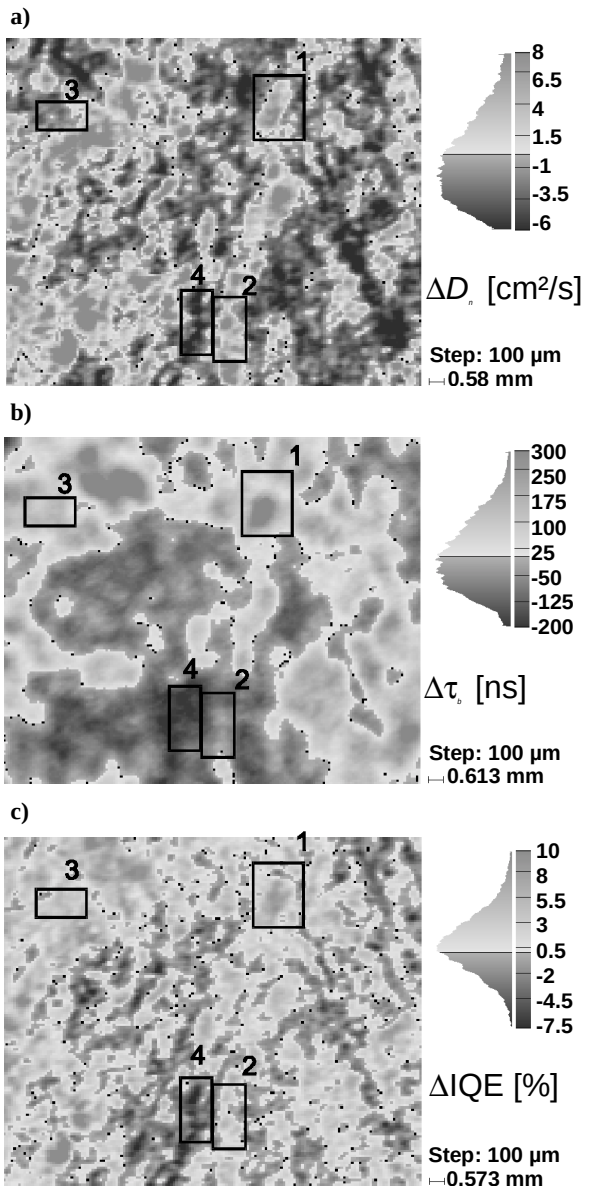

Figure 5a, b, c: Mapping of the difference to the mean value of the lifetime, the diffusion constant and the internal quantum efficiency respectively. The four marked regions indicate interesting areas for comparison.

4. CONCLUSIONS

The introduced method for deriving the minority charge carrier diffusion constant resolved in two dimensions is especially useful for silicon materials with low diffusion lengths where Basore conditions are satisfied. For other materials like EFG or Baysix regions with diffusion lengths $L_{diff} > d$ have to be excluded from calculations.

Scattering and recombination centers in RGS material have been investigated. Our results clarify, that these two defects are not always linked together. Regions with scattering defects can be recombination centers as well, but they do not necessarily have to.

The diffusion constant and therefore scattering centers are slightly dependent on hydrogen passivation.

More calculations of D_n will be carried out for all investigated materials in order to increase statistics and therefore the reliability of the calculated diffusion constants.

Further investigations on scattering and recombination effects will be performed before and after hydrogenation to clarify the influence of hydrogen passivation on the different types of defects.

5. ACKNOWLEDGEMENTS

This work was supported within the KoSi program by the German Bundesministerium für Wirtschaft (BMWi) under contract number 0329858J.

6. REFERENCES

[1] A. B. Sproul, M. A. Green and A. W. Stephens, Accurate determination of minority carrier- and lattice scattering-mobility in silicon from photoconductance decay, J. Appl. Phys. **72** (9), 4161 (1992)

[2] J.A. Eikelboom, C. Leguijt and A.R. Burgers, Separation of bulk and surface recombination rates in silicon wafers using a new microwave reflection technique, Proc. 12th EC PVSEC, Amsterdam 1994, 1782

[3] H. Lange, I. A. Schwirtlich, Ribbon Growth on Substrate (RGS) – A new approach to high speed growth of silicon ribbons for photovoltaics, J. Crystal Growth 104 (1990), 108-112

[4] P. Geiger, G. Kragler, G. Hahn, P. Fath, E. Bucher, Spatially Resolved Lifetime Investigations of Al- and P-Gettering in Combination with Remote Hydrogen Plasma Passivation in EFG Ribbon Silicon, Proc. 17th EC PVSEC Munich Germany 2001, VC3-4, to be published

[5] T. Pernau, M. Spiegel, P. Fath, E. Bucher, High Speed and High Accuracy IQE and L_{eff}-Mapping – A tool for Advanced Quality Control in the PV Industry, Proc. 17th EC PVSEC Munich Germany 2001, VD1-4, to be published

[6] P. A. Basore, Numerical Modeling of textured silicon solar cells using PC1D, IEEE Trans. Electron Devices **ED-37** (1990), 337

[7] G. Hahn, C. Zechner, M. Rinio, P. Fath, G. Willeke, E. Bucher, Enhanced carrier collection observed in mechanically structured silicon with small diffusion length, J. Appl. Phys. 86 (12), 7179 (1999)

[8] A. W. Stephens and M. A. Green, Minority carrier mobility of Czochralski-grown silicon by microwave-detected photoconductance decay, J. Appl. Phys. **74** (10), 6212 (1993)

[9] C. Häßler, H.-U. Höfs, S. Thurm, Electronic Activity of Inversion Channels: Exceptionally High Short Circuit Currents >30 mA/cm² on Small Grain Ribbon Growth on Substrate (RGS) Silicon, Proc. 16th EC PVSEC, Glasgow 2000